PHYSICAL REVIEW B **83**, 115324 (2011)

Exciton-exciton and exciton-phonon interactions in an interfacial GaAs quantum dot ensemble

G. Moody,[1,2] M. E. Siemens,[1,*] A. D. Bristow,[1,†] X. Dai,[1,‡] D. Karaiskaj,[1,§] A. S. Bracker,[3] D. Gammon,[3] and S. T. Cundiff[1,2,‖]

[1]*JILA, University of Colorado & National Institute of Standards and Technology, Boulder, Colorado 80309-0440, USA*

[2]*Department of Physics, University of Colorado, Boulder, Colorado 80309-0390, USA*

[3]*Naval Research Laboratory, Washington, DC 20375, USA*

(Received 2 August 2010; revised manuscript received 16 December 2010; published 23 March 2011)

Using optical two-dimensional Fourier transform spectroscopy, we report temperature- and excitation-density-dependent measurements of the homogeneous linewidth of the exciton ground-state transition in a single layer of interfacial GaAs quantum dots (QDs). We show that the homogeneous linewidth increases nonlinearly with temperature from 6 to 50 K and that the thermal broadening is well described by an activation term and offset. The absence of a phonon-activation peak in the two-dimensional spectra reveals that elastic scattering of excitons with acoustic phonons via virtual transitions between the ground and excited states significantly contributes to the thermal broadening. We find that the combination of increasing virtual activation energy and exciton-phonon coupling strength with decreasing QD size results in greater thermal broadening for excitons localized in smaller QDs. The homogeneous linewidth also exhibits a strong excitation-density dependence and is shown to increase linearly as the photon density increases from 2×10^{11} to 1×10^{12} photons pulse^{-1} cm^{-2} at 6 K. This trend is attributed to strong coupling of excitons within the same QD and is independent of the quantum-well exciton population density.

DOI: 10.1103/PhysRevB.83.115324 PACS number(s): 78.67.Hc, 78.47.nj, 63.22.−m

I. INTRODUCTION

The study of low-dimensional semiconductor systems provides insight into fundamental light-matter interactions that are relevant for applications based on coherent control and nonlinear processes. Semiconductor quantum dots (QDs) formed at interfacial fluctuations of a thin GaAs/$Al_{0.3}Ga_{0.7}$As quantum well (QW) are a model zero-dimensional system for investigating coherent exciton and carrier interactions because of their discrete energy-level structure,[1–4] narrow homogeneous linewidth,[5] large oscillator strength,[6,7] and defect-free growth process. The dephasing time (inversely proportional to the homogeneous linewidth) of the excitonic polarization is dependent on the QD surroundings, such as lattice temperature T_L, exciton population density, and material composition.

In higher-dimensional semiconductor systems, exciton-phonon interaction is an important mechanism for loss of coherence. In QDs the interaction with phonons has been expected to be suppressed because of the discrete density of states, resulting in the prediction of a phonon bottleneck.[8] Nonetheless, a strong thermal component of the homogeneous linewidth is observed; it has been suggested that at low temperatures the homogeneous linewidth of GaAs QDs is radiative-lifetime limited, while at higher temperatures thermal broadening is due to acoustic-phonon activation of the exciton into higher-lying states.[5] However, Fan *et al.* observed that population decay contributes weakly to thermal broadening and the dephasing can be described by a single decay rate, leading to a Lorentzian homogeneous line shape known as the zero-phonon line (ZPL).[9] More recently, several theoretical and experimental investigations have shown that elastic exciton-phonon coupling for interfacial[10] and self-assembled[11,12] QDs is the dominant contribution to the excitonic dephasing and results in a non-Lorentzian homogeneous line shape with broad sidebands superimposed onto the ZPL. Although it has been suggested that the discrepancy between the observed line shapes is due to differences in exciton confinement,[10] an investigation of the homogeneous line-shape temperature dependence will provide insight into the mechanisms contributing to the thermal broadening.

While a QD can be modeled as an atomiclike zero-dimensional system due to the discrete nature of the energy states, QDs differ from atomic systems because of intra- and inter-QD and QD-QW excitonic coupling. Consequently, many-body effects similar to those seen in QWs (Ref. 13) play a significant role in the coherent response of excitons localized within a QD. The homogeneous linewidth has been shown to increase linearly with excitation density,[9] however, this broadening is often undesired and investigations of the coherent response in QDs are performed at low excitation density. Coherent coupling in a small QD ensemble of individual, localized excitons in the low excitation-density regime[14] reveals that multiple excitons can couple via numerous mechanisms, including the Coulomb interaction, exchange interaction, and Förster coupling. Despite this strong evidence for exciton-exciton coupling in localized states, the dominant coupling mechanism is still undetermined.

In this paper we use optical two-dimensional Fourier transform spectroscopy (2DFTS) to study the temperature and excitation-density dependence of the homogeneous linewidth of a single layer of interfacial GaAs QDs. 2DFTS is an enhanced transient four-wave mixing (TFWM) technique that correlates the phase evolution of the nonlinear signal with the phases of the excitation pulses, which allows complicated spectra to be unfolded onto two dimensions.[15] We present measurements of the temperature dependence of the homogeneous linewidth at the line center of an inhomogeneously broadened QD ensemble in the temperature range of 6–50 K and show that our retrieved values agree with those obtained from independent investigations of single QDs.[16] The linewidth temperature dependence exhibits an activation-type behavior; however, lack of a phonon-activation peak

and the absence of acoustic-phonon sidebands in the 2D spectra suggest that an extension of the framework of the Huang-Rhys theory that includes virtual transitions to excited states[17] is a possible explanation for our observations of the ZPL thermal broadening. We measure the virtual activation energy and exciton-phonon coupling strength as a function of QD size and show that excitons localized in smaller QDs dephase more quickly. The ZPL width is also sensitive to the QD exciton population density and is independent of the QW exciton population, suggesting that excitation-induced dephasing is predominantly due to interactions of localized QD excitons. We provide evidence indicating that intra-QD excitonic coupling is the primary density-dependent dephasing mechanism.

II. SAMPLE AND EXPERIMENTAL TECHNIQUE

We study an epitaxially grown single GaAs QW 15 monolayers thick, corresponding to ≈4.2 nm, with 35-nm $Al_{0.3}Ga_{0.7}As$ barriers. An epitaxial-growth interruption wait time on the order of tens of seconds at the top $GaAs/Al_{0.3}Ga_{0.7}As$ interface results in monolayer width fluctuations in the QW thickness. These width fluctuations form islandlike features known as interfacial or "natural" QDs, shown as a schematic in Fig. 1(a). Upon optical excitation, delocalized excitons are created in the QW and localized excitons are created in the QD ensemble. The QD ensemble is inhomogeneously broadened because the sample has a distribution of QD sizes in the single GaAs layer. Excitons in the QW are inhomogeneously broadened due to averaging of the wavefunction over high-frequency fluctuations at the $Al_{0.3}Ga_{0.7}As/GaAs$ interface, which are inherent to the epitaxial-growth process.

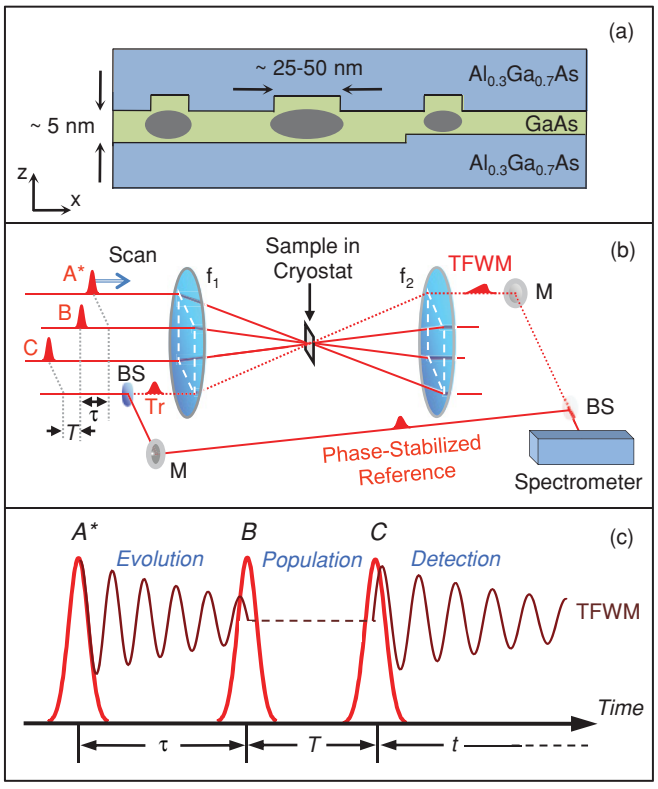

FIG. 1. (Color online) (a) Schematic diagram of the GaAs QD sample structure, (b) the two-dimensional Fourier transform spectroscopy experimental setup, and (c) the phase-stabilized excitation pulse sequence in the rephasing time ordering.

Localization of an exciton in a QD state increases the exciton binding energy because of greater electron and hole wave function overlap and decreases the homogeneous linewidth with respect to QW excitons. The wave functions of excitons generated in these regions are confined in the growth direction by the $GaAs/Al_{0.3}Ga_{0.7}As$ band mismatch (300 meV) and in the lateral directions by the monolayer difference in QW thickness, with an additional confinement energy of ≈10 meV based on the QD-QW peak height energy separation. The resulting three-dimensional confinement creates a model zero-dimensional system due to the defect-free growth process, which limits the number of nonradiative recombination sites in the sample.

The minimum QD size allowed for the existence of a bound exciton state is $\xi_0 = \pi\hbar/\sqrt{2MV_0}$ (which roughly coincides with the exciton Bohr radius), where M is the exciton mass and V_0 is the confining potential of the QD relative to the QW. If the lateral dimensions of a QD are 2–3 times ξ_0, then a splitting of states corresponding to excitons confined in the 2D QW and lower-energy excitons weakly bound within a zero-dimensional QD is observed.[18] Matching the energy eigenvalues obtained from a solution to Schrödinger's equation for a finite three-dimensional box, using $M = 0.18m_e^*$ and a binding potential of $V_0 = 10$ meV, to photoluminescence exitation (PLE) spectra gives a typical QD size in our sample of 36 nm. This value is two times ξ_0 for our sample and indicates that excitons in our QDs are weakly localized in the lateral dimensions.

While one-dimensional TFWM techniques can measure the homogeneous linewidth in the presence of inhomogeneous broadening in the photon echo geometry, prior knowledge of the nature of the broadening is required in order to correctly extract the homogeneous linewidth.[19] In contrast, 2DFTS has the advantage of being able to unfold a complicated TFWM spectrum onto 2D and allows for the measurement of the homogeneous and inhomogeneous linewidths simultaneously.

2DFTS is based on a three-pulse TFWM technique, where the excitation pulses have wave vectors $\mathbf{k}_a$, $\mathbf{k}_b$, and $\mathbf{k}_c$. The phase-stabilized excitation pulse sequence generates a complex multidimensional time-domain TFWM signal field that is emitted in the phase-matched direction $\mathbf{k}_s = -\mathbf{k}_a + \mathbf{k}_b + \mathbf{k}_c$. In the experiments discussed in this paper, the excitation pulse sequence is in the rephasing time ordering, where the conjugate pulse A^* arrives first and is followed by pulses B and C. The delay between pulses A^* and B is called the evolution time and is denoted τ, between pulses B and C is called the population time and is denoted T, and the emission time after the arrival of pulse C is denoted t. The complex rephased signal, $S_I(\tau,T,t)$, is heterodyne detected with a phase-stabilized reference and the excitation pulse delays are stepped with interferometric precision.

Figures 1(b) and 1(c) show the experimental setup and the rephasing excitation pulse sequence, respectively (for details of the apparatus, see Bristow *et al.*[20]). A mode-locked

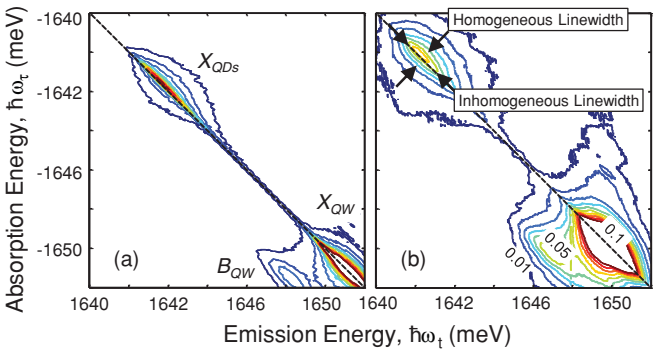

FIG. 2. (Color online) Amplitude 2DFT spectrum (normalized to the QW peak and truncated to emphasize the QD signal) of QW and QD ensemble for $T_L = 6$ K (a) and 50 K (b). The QW and QD homogeneous linewidths increase and the spectral features redshift with temperature.

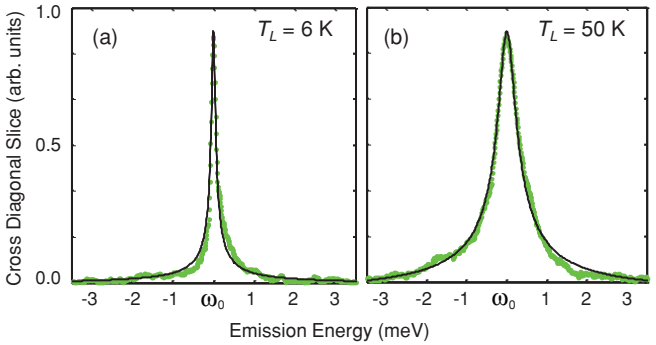

FIG. 3. (Color online) Cross diagonal slices (points) and $\sqrt{\text{Lorentzian}}$ fits (solid lines) at the inhomogeneous distribution line center of $|S_I(\omega_\tau, T, \omega_t)|$ for $T_L = 6$ K (a) and 50 K (b).

Ti:sapphire laser produces 100-fs pulses at a repetition rate of 76 MHz and at a tunable wavelength of ≈755 nm, which are incident on the sample in the box geometry. The excitation pulse spectrum is centered over the QD distribution and is broad enough to excite both the QD and QW excitons but not carriers in the continuum. The three excitation beams overlap in a circular spot with a diameter of 80 μm, encompassing $\approx 10^5$ QDs. The average power per beam incident on the sample is variable between 0.2 and 1.0 mW (2×10^{11} and 1×10^{12} photons pulse^{-1} cm^{-2}) and the polarization is set to colinear. The heterodyned signal is spectrally resolved with a resolution of 17 μeV as the time delay τ is scanned while keeping the delay T fixed. A Fourier transform of the signal with respect to τ produces a complex field $S_I(\omega_\tau, T, \omega_t)$, whose magnitude is plotted in Fig. 2 for an average excitation power of 1.0 mW. The absorption energy axis, $\hbar\omega_\tau$, is constructed by the Fourier transform of S_I with respect to τ, and the emission energy axis, $\hbar\omega_t$, is reconstructed through the detection method using spectral interferometry. The absorption axis is plotted as negative energy because the conjugate pulse A^* arrives at the sample first.

The TFWM signal radiated from a single layer of GaAs QDs is extremely weak and is often masked by pump scatter, which would appear along the diagonal of the spectra (dashed line in Fig. 2) because the pump is only self-coherent. To increase the signal-to-noise ratio, we use a four-position phase cycling scheme, where we toggle the phases of the excitation pulses by π at each delay step τ_i and add or subtract the subsequent spectra.[20,21] Using this technique, pump light scattered in the phase-matched direction will cancel and only the desired TFWM signal and reference remain.

The inhomogeneous and homogeneous linewidths, shown in Fig. 2, are obtained by fitting a cross-sectional slice along the diagonal and cross diagonal (perpendicular to the diagonal), respectively. Calculations based on the two-level optical Bloch equations with strong inhomogeneous broadening show that $|S_I(\omega_\tau, T, \omega_t)|$ is a Gaussian along the diagonal and a $\sqrt{\text{Lorentzian}}$ along the cross diagonal.[22] Figures 3(a) and 3(b) show $\sqrt{\text{Lorentzian}}$ fits to cross diagonal slices of $|S_I(\omega_\tau, T, \omega_t)|$ at the line center of the inhomogeneous distribution for $T_L = 6$ and 50 K, respectively. For all fits the largest error in the full width at half maximum (FWHM) between the experimental data and the $\sqrt{\text{Lorentzian}}$ is 5%. The diagonal fits and the absence of sidebands on the homogeneous line shapes will be discussed in the following section.

III. LINEWIDTH TEMPERATURE DEPENDENCE

The homogeneous linewidth (or equivalently, dephasing rate), γ, is related to population relaxation, Γ, and pure elastic dephasing processes, γ^*, by $\gamma = \frac{\Gamma}{2} + \gamma^*$. The population decay rate can be further divided into $\Gamma = \Gamma_{sp} + \Gamma_{nr}$, where Γ_{sp} and Γ_{nr} are the spontaneous and nonradiative population relaxation rates, respectively. The results described in this section were obtained for an average excitation power of 1.0 mW and $T = 200$ fs.

Figure 4(a) shows the absorption line shape obtained by projecting a 2D amplitude spectrum onto the absorption axis for $T_L = 6$ and 50 K, with the line center marked by the vertical arrows. With an increase in temperature, the band-gap decrease redshifts the inhomogeneous distribution. Although the simulations mentioned previously use Gaussian inhomogeneous broadening, we observe an asymmetric inhomogeneous line shape with a tail on the high-energy side of the distribution. In photoluminescence, a similar asymmetry was observed and is attributed to excitons with a statistical wave-vector distribution of finite width at approximately $\mathbf{K} = 0$ recombining within the QDs.[23] The optical density—which is proportional to the absorption spectrum—was derived by Schnabel *et al.* and calculated by Leosson *et al.* for a disordered potential with average energy E_0 to be[24]

$$\alpha(E) \propto \frac{1}{2\eta}\left[1 + \text{erf}\left(\frac{E - E_0}{\sigma_E} - \frac{\sigma_E}{2\eta}\right)\right] e^{\left(\frac{\sigma_E}{2\eta}\right)^2 - \frac{E - E_0}{\eta}}, \quad (1)$$

where erf is the error function [$\text{erf}(x) = 2/\sqrt{\pi}\int_0^x e^{-x'^2}\,dx'$], σ_E is the FWHM of the potential variation, and $\eta = \hbar^2\Delta\mathbf{K}^2/2M$ is defined to be the localization energy parameter derived for a wave-vector uncertainty $\Delta\mathbf{K}$ and exciton mass M.

The model fits our experimental data well for both the low- and high-temperature regimes and is consistent with our typical QD size being twice as large as the localization parameter ξ_0. This result is direct evidence that excitons bound within these interfacial QDs are only weakly localized in three

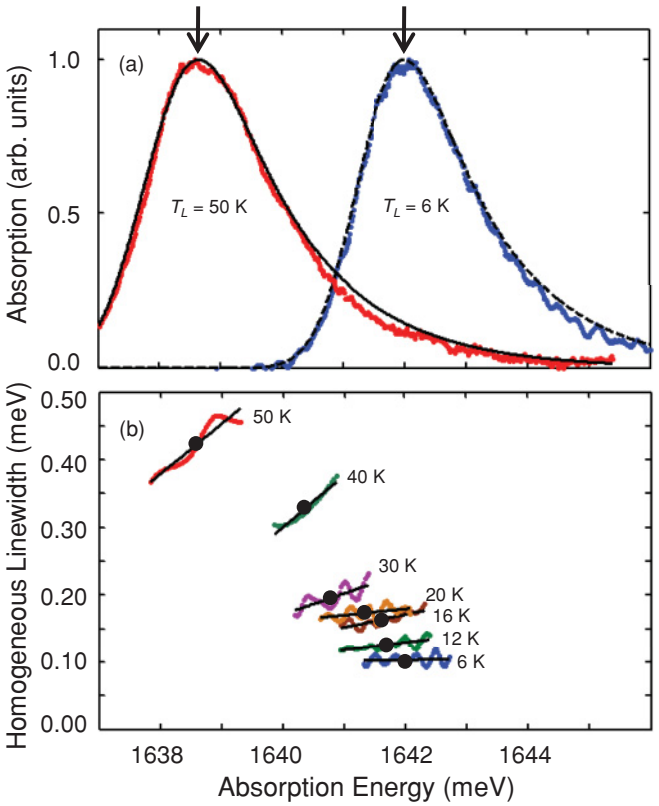

FIG. 4. (Color online) (a) The asymmetric absorption line shape, obtained by projecting the 2D amplitude spectrum onto the absorption axis, is inhomogeneously broadened and is fit with Eq. (1) for T_L = 6 K (dashed line) and 50 K (solid line). The line center is indicated by the vertical arrows. (b) The homogeneous linewidths across the inhomogeneous distribution for an average excitation power of 1.0 mW are shown as a function of temperature. The line center is indicated by the solid circles.

dimensions, which has strong implications on the power and temperature dependence of the homogeneous linewidth.

Figure 4(b) shows the homogeneous linewidth across the inhomogeneous distribution for varying temperatures in the range between $T_L = 6$ and 50 K, with the line center marked by the solid circles. The homogeneous linewidth increases linearly with increasing energy (decreasing QD size) across the inhomogeneous distribution for all temperatures when using an average excitation power of 1.0 mW. Oscillations in the linewidths are due to time truncation artifacts of the TFWM signal and are more pronounced at lower temperatures, where the signal dephases more slowly. At each temperature a linear fit is performed and the values used are taken from these fits.

The temperature dependence of the homogeneous linewidth at the line center is shown in Fig. 5. Thermal broadening of the homogeneous linewidth for excitons in QDs has been modeled by considering the probability of phonon absorption and subsequent excitation of the exciton to higher-lying states,[5]

$$\gamma_\mu(T) = \gamma_\mu^* + \sum_{\nu>\mu} \gamma_{\mu\nu} n(E_{\mu\nu}, T), \tag{2}$$

where $n(E_{\mu\nu}, T) = [e^{E_{\mu\nu}/k_b T} - 1]^{-1}$ is the Bose-Einstein distribution that describes the number of phonons at an

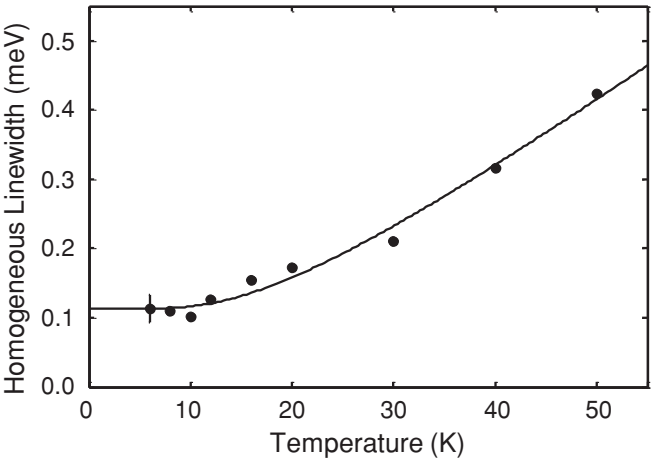

FIG. 5. Temperature dependence of the homogeneous linewidth measured at line center for an average excitation power of 1.0 mW and $T = 200$ fs, with a representative error bar (high-low values) determined from repeating the measurement at $T_L = 6$ K. Equation (2) is fit to the data using an activation energy of $E_{12} = 4.4 \pm 0.8$ meV and an offset of $\gamma_1^* = 0.11 \pm 0.01$ meV. The absence of an activation peak in the 2D spectra reveals that the dominant thermal broadening mechanism is *elastic* exciton-phonon scattering.

energy $E_{\mu\nu}$. The first term in Eq. (2) represents temperature-independent dephasing, while the second term is due to activation of the exciton from state μ to a higher-lying energy state.

We use a single term from the sum in Eq. (2) to fit the data, plotted as the solid line in Fig. 5, and extract an activation energy of $E_{12} = 4.4 \pm 0.8$ meV and an offset of $\gamma_1^* = 0.11 \pm 0.01$ meV. The offset is predominantly a result of excitation-induced dephasing and is discussed in the next section. A solution to Schrödinger's equation, mentioned previously, as well as PLE spectra reveal discrete energy levels with a separation in the range of E_{12}. Although this model fits the data well and the extracted activation energy is consistent with the one-phonon population activation mechanism, we rule out this possibility because we do not observe an activation peak in the 2D spectra for long T (additional data not shown). For short T, population activation would increase the homogeneous linewidth but would not appear as an additional peak in the 2D spectra because the phase evolves during τ. By recording 2D spectra for long T, we can observe incoherent population dynamics because the phase does not evolve during T. If activation was the cause of the thermal broadening, it would appear as a 4.4 ± 0.8 meV blueshifted peak from the line center along the emission axis.

The absence of an activation peak signifies that the thermal broadening is due to exciton population decay and pure dephasing processes. Extrinsic dephasing processes resulting from a fluctuating electrostatic potential have been investigated for self-assembled InAs QDs;[25,26] however, we believe that this mechanism is not important because our sample is grown using a defect-free epitaxial growth process that eliminates charge carrier trapping sites.[2,3] Additionally, filtering the excitation spectrum to ensure that neither QW excitons nor carriers are generated has no apparent effect on the measured QD linewidths.

Theoretical and experimental studies show that, at elevated temperatures, exciton population decay contributes only weakly to the increase in the dephasing rate[9,17] and that elastic exciton-phonon coupling dominates the excitonic dephasing.[9–12,17] Calculations based on the Huang-Rhys theory using linear coupling of excitons to acoustic phonons predict the appearance of broad acoustic-phonon sidebands on a narrow temperature-independent ZPL. However, a model extending the framework of the Huang-Rhys theory to include quadratic exciton-phonon coupling incorporates thermal broadening of the ZPL and predicts that the dephasing is strongly dependent on the relevant phonon energies and the QD size.[17] In this model, the dephasing rate increases linearly with temperature when the energy of the acoustic phonons is much less than the energy separation between the ground and first excited states in the QD and only virtual processes within the exciton ground state need to be considered. At higher temperatures, when the thermal energy approaches the QD energy-level separation, virtual transitions from the ground state→excited state→ground state contribute substantially to the dephasing and a nonlinear temperature dependence is expected.[17] The appearance of acoustic-phonon sidebands on the ZPL occurs only for a large Huang-Rhys factor, which characterizes the exciton-phonon coupling strength and increases with confinement. Fan *et al*. measure a single decay rate leading to a Lorentzian ZPL without sidebands in a GaAs QD system,[9] while Peter *et al*. observe sidebands in μ-PLE spectra in a similar system[10] and Borri *et al*. report line shapes with strong sidebands in InAs QDs.[27] The absence of sidebands in the line shapes reported by Fan *et al*. can be attributed to weaker confinement in larger QDs.[28]

In the GaAs QDs discussed here with lateral dimensions of ≈40 nm, phonons with energies below 1 meV couple most strongly to excitons.[10,17] In this system with weak confinement, the exciton-phonon coupling strength responsible for acoustic-phonon sidebands is dramatically reduced and sidebands are not observed on our line shapes up to $T_L = 50$ K. Weak exciton confinement and ground-to-excited state energy-level separation of a few meV result in a linear temperature dependence of the dephasing rate for $T_L < 20$ K. At elevated temperatures, the thermal broadening is well described by the same activation term that is used to fit the data in Fig. 5. These results are qualitatively consistent with those reported by Takagahara. Quantitatively, our reported ZPL width of ≈300 μeV at 50 K (after subtracting the broadening from excitation-induced dephasing) falls between ≈200 μeV at 50 K reported by Fan *et al*. and ≈450 μeV at 25 K reported by Peter *et al*. While Peter *et al*. phenomenologically broadened the ZPL in their theoretical model, Fan *et al*. applied Takagahara's theory with good agreement. Comparison of our results to those obtained by Fan *et al*. allows us to conclude that the thermal broadening in these QDs is dominated by virtual transitions of the ground-state exciton via elastic exciton-phonon coupling, rather than inelastic phonon-assisted activation of the exciton population to higher-lying QD states.

We measure the homogeneous linewidth temperature dependence as a function of energy offset from the line center (QD size) and fit the thermal broadening with Eq. (2). Figure 6 shows that the virtual activation energy, E_{12} (solid line), and the exciton-phonon coupling strength prefactor, γ_{12} (dashed line), both increase with increasing exciton energy (decreasing QD size) across the inhomogeneous distribution. An increase in E_{12} is a direct result of the ground-to-excited state energy separation increasing with decreasing QD size. A solution to Schrödinger's equation, described in Sec. II, shows that E_{12} changes by ± 1.0 meV for a change in exciton energy of ± 0.8 meV about the line center, which agrees well with our measured values of E_{12}.

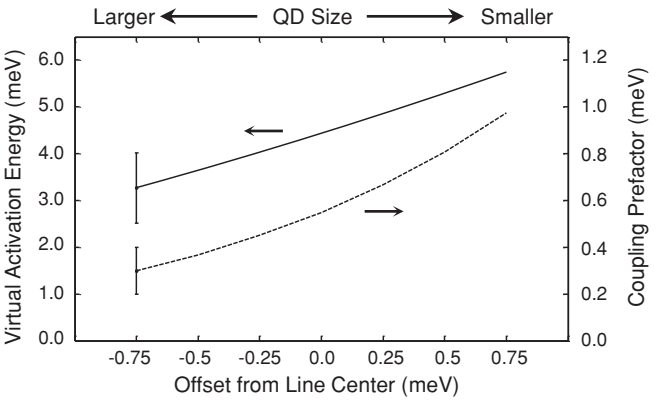

FIG. 6. The virtual activation energy (solid line) and exciton-phonon coupling prefactor (dashed line), obtained from fitting Eq. (2) to the homogeneous linewidth temperature dependence, increase across the inhomogeneous distribution for an average excitation power of 1.0 mW.

A larger E_{12} for smaller QDs would indicate weaker thermal broadening; however, we observe an increase of the slope of the linear fits to the homogeneous linewidth with temperature, shown previously in Fig. 4. Consequently, greater thermal broadening for smaller QDs is a result of a larger exciton-phonon coupling prefactor, shown as the dashed line in Fig. 6. The effect of γ_{12} dominates the effect of E_{12} and is consistent with Takagahara's work,[17] which predicts greater exciton-phonon coupling for smaller QDs, and therefore a stronger temperature dependence.

IV. EXCITATION-INDUCED DEPHASING

The inset of Fig. 7 shows the excitation-induced dephasing (EID) behavior of the homogeneous linewidth at the line center of the inhomogeneous distribution measured at $T_L = 6$ K. As the average excitation power decreases to zero, the linewidth decreases linearly to a value of $\gamma = 30.6$ μeV. This zero excitation-density value is consistent with previous studies on single QDs[3,5,9] and confirms that the measured homogeneous linewidth of a QD ensemble using 2DFTS is similar to single QD values. At low temperature and extrapolating to zero excitation density, dephasing from phonon scattering and many-body interactions is negligible. Furthermore, the low-strain growth process minimizes nonradiative recombination defect sites. Under these assumptions, the extrapolated homogeneous linewidth, γ, is radiative lifetime broadened with a lifetime of $1/\Gamma_{sp} = 1/(2\gamma) = 68$ ps.

The line-center homogeneous linewidth power dependence measurements were repeated using a pulse shaper to spectrally filter the excitation pulses such that QW excitons were not generated, and we observed no change in the EID of the

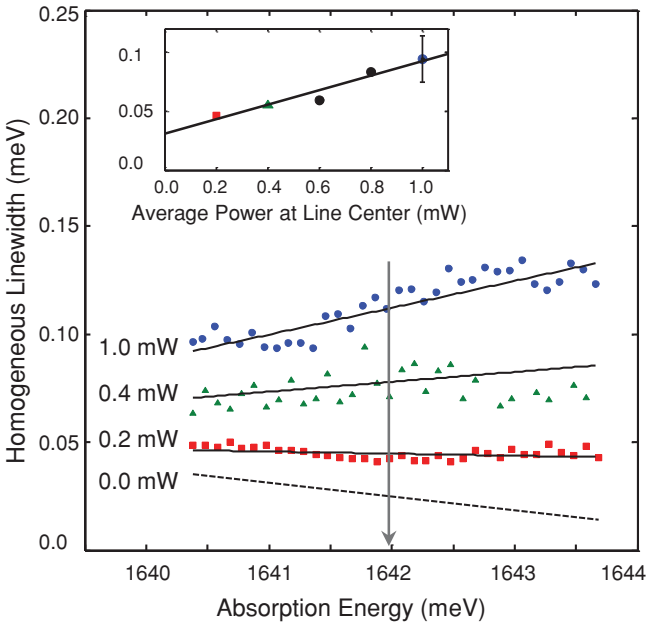

FIG. 7. (Color online) The homogeneous linewidth across the inhomogeneous distribution at $T_L = 6$ K for average excitation power of 1.0 mW (circles), 0.4 mW (triangles), 0.2 mW (squares), and extrapolated 0.0 mW (dashed line). The gray vertical arrow indicates the line center of the inhomogeneous distribution. Inset: power dependence of the QD homogeneous linewidth at line center at $T_L = 6$ K. Extrapolating to zero excitation density results in a homogeneous linewidth of $\gamma = 30.6$ μeV, corresponding to a radiative lifetime of 68 ps.

QD ensemble (not shown). This is an interesting result: EID effects play a significant role in the dephasing of QD excitons as shown in the inset of Fig. 7, but the QW excitons have a negligible effect; therefore, this many-body behavior is governed primarily by intra- and inter-QD excitonic couplings. Generating multiple excitons in a single QD energy state is possible because of spin degeneracy; we can neglect the creation of excitons in higher-lying energy states because of the absence of additional peaks in the 2D spectra.

Figure 7 shows the homogeneous linewidth variation across the inhomogeneous distribution at $T_L = 6$ K for three different average excitation powers and an extrapolation to zero. Under similar assumptions as those above pertaining to the nature of the broadening at $T_L = 6$ K and zero excitation, the extrapolated zero excitation-density linewidth values are radiative lifetime broadened and are proportional to Γ_{sp}. The negative slope is consistent with the higher-energy (smaller) QDs having a smaller transition dipole moment (proportional to $\sqrt{\Gamma_{sp}}$).[7,29] With increasing power, the overall homogeneous linewidth increases and the slope flips from negative to positive. This behavior suggests that multiple excitons are generated within a given QD, and the coupling between these excitons increases with decreasing QD size due to greater exciton-exciton wave-function overlap.

Transient coherent nonlinear spectroscopy has revealed[14] that individual excitonic transitions couple to form biexcitons, but intra- versus inter-QD coupling mechanisms have not been determined. While we cannot directly distinguish between intra- and inter-QD coupling in our experiment, we observe a redshifted biexciton feature parallel to and stronger than the exciton feature in cross-linear polarized[30] 2DFT spectra (not shown). The elongation and narrow width of the biexciton peak reveal that these biexcitons form from two spatially overlapping excitons. Combining this observation with the evidence of an increased dephasing rate for higher-energy QDs, we suggest that the dominant EID mechanism for a single layer of an interfacial GaAs QD ensemble is intra-QD excitonic coupling. This result is further supported by recent microscopic nonlinear imaging measurements.[31]

V. SUMMARY

We use two-dimensional Fourier transform spectroscopy to measure the temperature and excitation-density dependence of the homogeneous linewidth of excitons in interfacial GaAs QDs. The observed inhomogeneous and homogeneous line shapes suggest that our QDs weakly localize the exciton in three dimensions, rather than strong, atomiclike binding expected from an ideal QD system. The thermal broadening of the homogeneous linewidth, combined with the absence of activation peaks in the 2D spectra, reveal that elastic exciton-phonon scattering is the dominant mechanism. Virtual transitions between the ground and excited states contribute significantly to the exciton dephasing, which explains the activationlike thermal broadening we observe. Excitation-induced effects are shown to strongly influence the homogeneous linewidth independence of the QW exciton population, having a greater effect on higher-energy QDs. These results suggest that intra-QD exciton coupling is the dominant EID mechanism, which is also supported by the observation of a strong biexciton feature in the cross-linearly polarized spectra.

ACKNOWLEDGMENTS

This work was supported by the National Science Foundation, the (U.S.) Department of Energy, and the Chemical Sciences, Geosciences, and Biosciences Division Office of Basic Energy Sciences. M.E.S. acknowledges funding from the National Academy of Sciences and National Research Council.

*Present address: Department of Physics and Astronomy, University of Denver, Denver, CO 80208-6900.
†Present address: Department of Physics, West Virginia University, Morgantown, WV 26506-6315.
‡Present address: Department of Physics, Tsinghua University, Beijing 100084, China.
§Present address: Department of Physics, University of South Florida, Tampa, FL 33620.
‖cundiff@jila.colorado.edu

[1] A. Zrenner, L. V. Butov, M. Hagn, G. Abstreiter, G. Böhm, and G. Weimann, Phys. Rev. Lett. **72**, 3382 (1994).

[2]K. Brunner, G. Abstreiter, G. Böhm, G. Tränkle, and G. Weimann, Appl. Phys. Lett. **64**, 3320 (1994).
[3]H. F. Hess, E. Betzig, T. D. Harris, L. N. Pfeiffer, and K. W. West, Science **264**, 1740 (1994).
[4]D. Gammon, E. S. Snow, and D. S. Katzer, Appl. Phys. Lett. **67**, 2391 (1995).
[5]D. Gammon, E. S. Snow, B. V. Shanabrook, D. S. Katzer, and D. Park, Science **273**, 87 (1996).
[6]L. C. Andreani, G. Panzarini, and J.-M. Gérard, Phys. Rev. B **60**, 13276 (1999).
[7]J. R. Guest, T. H. Stievater, X. Li, J. Cheng, D. G. Steel, D. Gammon, D. S. Katzer, D. Park, C. Ell, A. Thränhardt, G. Khitrova, and H. M. Gibbs, Phys. Rev. B **65**, 241310(R) (2002).
[8]U. Bockelmann and G. Bastard, Phys. Rev. B **42**, 8947 (1990).
[9]X. Fan, T. Takagahara, J. E. Cunningham, and H. Wang, Solid State Commun. **108**, 857 (1998).
[10]E. Peter, J. Hours, P. Senellart, A. Vasanelli, A. Cavanna, J. Bloch, and J.-M. Gérard, Phys. Rev. B **69**, 041307(R) (2004).
[11]L. Besombes, K. Kheng, L. Marsal, and H. Mariette, Phys. Rev. B **63**, 155307 (2001).
[12]P. Borri, W. Langbein, U. Woggon, V. Stavarache, D. Reuter, and A. D. Wieck, Phys. Rev. B **71**, 115328 (2005).
[13]Y. Z. Hu, R. Binder, S. W. Koch, S. T. Cundiff, H. Wang, and D. G. Steel, Phys. Rev. B **49**, 14382 (1994).
[14]W. Langbein and B. Patton, Opt. Lett. **31**, 1151 (2006).
[15]S. T. Cundiff, T. Zhang, A. D. Bristow, D. Karaiskaj, and X. Dai, Acc. Chem. Res. **42**, 1423 (2009).
[16]N. H. Bonadeo, J. Erland, D. Gammon, D. Park, D. S. Katzer, and D. G. Steel, Science **282**, 1473 (1998).
[17]T. Takagahara, Phys. Rev. B **60**, 2638 (1999).
[18]H. Castella and J. W. Wilkins, Phys. Rev. B **58**, 16186 (1998).
[19]S. T. Cundiff, Opt. Express **16**, 4639 (2008).
[20]A. D. Bristow, D. Karaiskaj, X. Dai, T. Zhang, C. Carlsson, K. R. Hagen, R. Jimenez, and S. T. Cundiff, Rev. Sci. Instrum. **80**, 073108 (2009).
[21]R. R. Ernst, G. Bodenhausen, and A. Wokaun, *Principles of Nuclear Magnetic Resonance in One and Two Dimensions* (Clarendon, Oxford, UK, 1988).
[22]M. E. Siemens, G. Moody, H. Li, A. D. Bristow, and S. T. Cundiff, Opt. Express **18**, 17699 (2010).
[23]R. F. Schnabel, R. Zimmermann, D. Bimberg, H. Nickel, R. Lösch, and W. Schlapp, Phys. Rev. B **46**, 9873 (1992).
[24]K. Leosson, J. R. Jensen, W. Langbein, and J. M. Hvam, Phys. Rev. B **61**, 10322 (2000).
[25]A. Berthelot, I. Favero, G. Cassabois, C. Voisin, C. Delalande, Ph. Roussignol, R. Ferreira, and J. M. Gérard, Nat. Phys. **2**, 759 (2006).
[26]I. Favero, A. Berthelot, G. Cassabois, C. Voisin, C. Delalande, Ph. Roussignol, R. Ferreira, and J. M. Gérard, Phys. Rev. B **75**, 073308 (2007).
[27]P. Borri, W. Langbein, S. Schneider, U. Woggon, R. L. Sellin, D. Ouyang, and D. Bimberg, Phys. Rev. Lett. **87**, 157401 (2001).
[28]D. Gammon, E. S. Snow, B. V. Shanabrook, D. S. Katzer, and D. Park, Phys. Rev. Lett. **76**, 3005 (1996).
[29]L. C. Andreani, G. Panzarini, and J.-M. Gérard, Phys. Status Solidi A **178**, 145 (2000).
[30]A. D. Bristow, D. Karaiskaj, X. Dai, R. P. Mirin, and S. T. Cundiff, Phys. Rev. B **79**, 161305(R) (2009).
[31]J. Kasprzak, B. Patton, V. Savona, and W. Langbein, Nat. Photonics **5**, 57 (2011).